Study on Reinforced Modification of Polylactic Acid by New Hyperbranched Polyamide

Jianjian Sun
Beijing Technology and Business University
Yansong Huang
Beijing Technology and Business University
Yu juan Jin (jinyujuan@th.btbu.edu.cn)
Beijing Technology and Business University https://orcid.org/0000-0001-7366-5810
Lu Wang
Beijing Technology and Business University
Huafeng Tian
Beijing Technology and Business University

Research Article

Keywords: Polylactic acid, Hyperbranched Polyamide, reinforcing

Posted Date: September 30th, 2021

DOI: https://doi.org/10.21203/rs.3.rs-942988/v1

Abstract

In order to achieve enhanced physical performance of polylactic acid (PLA), the hyperbranched polyamide (HBPA) was synthesized by "one-step" as raw materials, and added as a modifier to the PLA matrix. The HBPA/PLA blend was prepared through the twin screw extrusion process and the injection molding process. The results showed that, compared with pure PLA, the tensile strength of HBPA/PLA blends increased by 41.8% while the elongation at break and the impact strength basically unchanged. The addition of HBPA does not affect the glass transition temperature (Tg) and crystallization of PLA significantly, but can improve the thermal deformation temperature of PLA. HBPA acted as a nucleant for PLA during iso-temperature crystallization. HBPA could form hydrogen bonds and chemical crosslinks with PLA, thus exhibits excellent reinforcing effect for PLA.

1 Introduction

As is well known, traditional petroleum-based plastics were difficult to decompose and non-biodegradable, so it was easy to cause serious "white pollution" and a series of environmental problems after being abandoned, which would eventually lead to global environmental problems and energy crises. Bio-based materials derived from animals and plants can not only reduce environmental pollution, but also reduce dependence on limited resources such as oil and coal, which was in line with sustainable development strategies. Therefore, academy and industry have shown great interest in the development of commodities made of biodegradable and renewable materials, and bio-based materials had become a hot spot for development today [1–5].

Polylactic acid (PLA) was extracted from renewable plant resources (such as corn, cassava, etc.). PLA had good biodegradability, and the production process was pollution-free. Moreover, it can be completely degraded by microorganisms under specific conditions in nature, finally, generated carbon dioxide and water. It did not pollute the environment, and can reduce the problems of "oil shortage" and "white pollution", so it was an ideal green polymer material. The main advantage of PLA lay in its environmental friendliness and ease of processing. It can be processed in a variety of processing methods such as extrusion, spinning, biaxial stretching, injection and blowing molding. Products made of PLA possess biodegradability, biocompatibility, good gloss, transparency, hand feel and heat resistance, but PLA was a linear polymer because it had no active side chain groups. It was difficult to modify its surface or body. In addition, polylactic acid had several obvious defects, such as brittleness, poor thermal stability and low crystallization rate, low heat distortion temperature [6–10], and compared with other aliphatic polyesters, the melt viscosity of PLA had low strength [11]. In order to be used in a wide range of products, methods such as copolymerization [12–13] and blending [14–18] and additives [17–20] have been reported to improve its strength and brittleness. Zhang et al. [21] used citric acid to modify calcium carbonate to improve the mechanical properties of the polylactic acid composite material. Li et al. [22] used KH570 silane coupling agent to modify silica and used it to reinforce polylactic acid materials.

In the past thirty years, hyperbranched polymer (HBP) had been a hot spot for additive modification due to its special organic-inorganic hybrid three-dimensional structure. HBP had a lot of branching points and low viscosity. The molecular chain of HBP was not easy to entangle. In addition, the end of the hyperbranched polymer had a large number of functional groups[23–27]. HBP with different properties can be prepared by adjusting the type and quantity of functional groups. The synthesis of hyperbranched polymers was mainly based on ring-opening polymerization and condensation polymerization. Functional groups at the ends of hyperbranched polymers can form a large number of hydrogen bonds and chemical crosslinking reactions with polymer groups[25–33]. With the development of research on HBP synthesis by scientific researchers, it can be directly prepared and synthesized through the "one-step method" .

In this work, hyperbranched polyamide with high activity was designed and synthesized, and it was used for the modification of PLA. The results showed that the physical and mechanical properties of PLA had been successfully enhanced. The degradable PLA bio-based material with improved performance exhibited both important scientific significance and broad application prospects.

2 Experimental

2.1 Materials

PLA (REVODE110, = 3.5×10^5 g · mol^{-1}, DI = 2.5) was purchased from Zhejiang Haizheng Biomaterials Co., Ltd. Trimesoyl chloride (TMC), anhydrous sodium carbonate and p-phenylenediamine (MSDS) were purchased from Shanghai Macleans Biochemical Technology Co., Ltd. Acetone was purchased from Beijing Chemical Reagent Company.

2.2 Synthesis of HBPA

The three-necked flask, partial pressure funnel, stirring paddle and beaker were washed with deionized water and dried before they were used. Poured 300ml of acetone into a 500ml three-necked flask, used an electronic balance to weigh 6.64g trimesoyl chloride and dissolved it in the acetone, turned on the stirring paddle to make it quickly dissolve, stirring at 120rpm, weighed 3.18g anhydrous sodium carbonate and 5.41g P-phenylenediamine and dissolved them into 100ml of 80^{o}C deionized water. After they were completely dissolved, the solution would be reddish brown. Added the reddish-brown solution dropwise to the three-necked flask through a partial pressure funnel. The solution in the three-necked flask quickly turned into a green turbid solution, and the mixture was heated in water at 20^{o}C for 6 hours. After the reaction, the green suspension was suction filtered, then the green solid obtained was washed with acetone 3 times and then washed with deionized water above 80^{o}C 3 times, and suction filtered several times to removed small molecular substances. Finally, it was placed in a vacuum drying oven at 80^{o}C for 12 hours to obtain a hyperbranched polyamide.

2.3 Preparation of the PLA/HBPA blends

PLA was dried at 80°C for 6 h before mixing with HBPA. PLA and HBPA with different contents were blended through a twin-screw extruder (CTE-35, Cobelon Coya Machinery Co., Ltd). The temperature of each zone of the twin-screw extruder was set to 140^{o}C, 145^{o}C, 150^{o}C, 150^{o}C, 145^{o}C, 140^{o}C, respectively. The PLA/HBPA blends were then cooled down before cutting into granule using a stock cutter (YH-2, SWP, Zhangjiagang Leyu Yuanhang Machinery Factory). The standard splines were prepared by an injection moulding machine (TY400, HangZhou DaYu Machinery Co., Ltd). The injection temperature was set to 170^{o}C, and the injection pressure was 50 bar.

2.4 Characterization

Samples were mixed with KBr at a weight ratio of 1:100 and processed into pellets for the use in Fourier transform infrared (FTIR) measurements. The scanning wavelength range of FTIR spectroscopy (Nicolet8700, Thermo Electron, USA) was set to be 4000 cm^{-1}-500 cm^{-1}. The resolution was set to 8 cm^{-1}. The scan number was 32.

An NMR spectrometer (Agilent NMR Magnet) was used to record ^{1}H high-resolution one-dimensional NMR spectra in dimethyl sulfoxide (DMSO) at room temperature.

Gel permeation chromatography (GPC) (DAWN HELEOS-II, Wyatt, USA) was carried out using N,N-Dimethylformamide (DMF) as the solvent. The concentration was 1mg mL^{-1}. Calibration was performed using polystyrene standards.

In the circulatory system, put the sample in chloroform at 60℃ for heating and refluxing to dissolve for 6h, then take it out and dry it at 80℃ for 8h, calculate the gel content () according to Eq. (1):

$$a = \frac{m_2}{m_1} \times 100\% \qquad (1)$$

In the formula: m_1 and m_2 are the mass of the sample before and after dissolution, in mg.

Rheological characterization of PLA/HBPA blends was tested by Rotational rheometer (MCR302, Anton Paar GmbH). The thickness of the test sample was 1mm, the temperature was set to 170°C, and the test was performed after the sample was melted. The initial value of the angular frequency was set to 0.1rad/s, and the final value was 100rad/s. The change rule was a logarithmic change.

The crystallization process of PLA was observed under polarized optical microscope(POM) (CBX51, Olympus). A small amount of sample was placed on a hot stage, heated to 200 ° C at a heating rate of 50 ° C /min and stayed at 200 ° C for 5 min to eliminate the thermal history, then cooled to 120 ° C at a cooling rate of 10 ° C / min and stayed at 120 ° C for 30 min. During the process, the iso-thermal crystallization processes were observed.

The fractured surfaces of impact specimens were observed under scanning electron microscopy (SEM) (QUATA250, FEI, USA). Before SEM, gold spraying was performed with a working voltage of 15 kV.

The differential scanning calorimeter (DSC) (Q100, TA, USA) was measured under the protection of nitrogen gas. The sample (5.0–10.0 mg) was heated from room temperature to 200 ^{o}C, pre-annealed at 200 ^{o}C for 3 min, followed by cooling to 20 ^{o}C at 20 ^{o}C /min and pre-annealed at 20 ^{o}C for 3 min, then reheated to 200^{o}C at 20 ^{o}C /min. Recorded and saved the DSC curve.

Thermogravimetric analyais (Q50, TA, USA) of the PLA/HBPA blends were measured under the protection of N_2 gas. Samples were heated from room temperature to 700 ^{o}C at 20 ^{o}C /min.

Characterization of Heat Deflection Temperature (HDT) was tested by HDT□VICAT Testing Machine (ZWK1302-B, MTS SYSTEMS (CHINA) CO., LTD.) according to the D648-07 standard, the temperature of the standard sample under the specified load and deformation, the heating rate was 120℃/h.

Tensile strength and elongation at break of the blends were tested by a computer-controlled electronic universal testing machine (CMT6104, MTS Industry System Co., Ltd., Shenzhen, Guangdong Province, PR China) according to ISO527.2 Standard. The tensile rate was chosen to be 20 mm/min. The size of the spline was dumbbell shaped spline, L = 150 mm, d = 4 mm.

Impact strength was tested by an electronic Izod impact testing machine (XJUD-5.5, Chengde Jinjian Testing Instrument Co., Ltd., Chengde, Hebei Province, PR China). The size of the spline without gaps was determined according to the ISO180:2000: 80 mm×10 mm×4 mm. The impact energy of the pendulum was 2 J.

3 Results And Discussion

3.1 FTIR characterization of HBPA

The HBPA was synthesized by adding MSDS deionized water solution dropwise to TMC acetone solution in a 20 ℃ water bath. As shown in Fig. 2 (a), the stretching vibration absorption peak of C-Cl bond at 703cm^{-1} in the TMC infrared curve, the absorption peaks at 1592 cm^{-1} and 1755 cm^{-1} were C = O double bonds. The N-H bond stretching vibration absorption peaks were located at 3201 cm^{-1}, 3303 cm^{-1}, and 3374 cm^{-1}, while 3356 cm^{-1} in HBPA was the newly generated N-H bond stretching vibration absorption peak. The hydrogen bond association interaction in a large number of amino groups at the terminal was the reason that the absorption peak becomes wider and smoother. 1313cm^{-1} and 1246cm^{-1} were newly formed C-N bonds, which were also accompanied by the disappearance of C-Cl bonds. Therefore, it proved that the hyperbranched polymer containing amide bond was successfully synthesized.

3.2 ^{1}H-NMR characterization of HBPA

Figure 2(b) was the ^{1}H-NMR spectrum of HBPA. It can be seen that there were at least seven different types of hydrogen atoms, of which δ 10.70 and 10.06 ppm were the characteristic peaks of hydrogen atoms on the amide bond (CONH), δ 8.71, 7.87, 7.48, 6.58 ppm were the characteristic peaks of hydrogen atoms on the benzene ring at different levels, and the characteristic peak at δ 2.52 ppm was the characteristic peak of hydrogen atoms on the terminal amino group (NH_2) of HBPA. The various types of hydrogen atoms also verify the successful synthesis of HBPA.

3.3 GPC characterization of HBPA

GPC test results showed that the number average molecular weight (M_n) of HBPA was 1.157×10^4 and 3.700×10^3, and the weight average molecular weight (M_w) was 4.738×10^4 and 1.185×10^4. It was known that there were two repeating units $C_9H_3O_3$ and $C_6H_6N_2$ in HBPA, and the molecular weights were 159 and 106, respectively. By calculation, the number average molecular weight of the first generation HBPA was 480, the second, third, fourth and fifth generations were 1596, 3828, 8292 and 17220 respectively. Therefore, it can be concluded that the HBPA synthesized by the one-pot method contained three and four generations.

3.4 FTIR characterization of PLA/HBPA blends

FTIR was a direct and common method to analyze the interaction between two polar groups. The FTIR spectra of the HBPA/PLA blend was shown in Fig. 3(a). Obviously, in the range of 3200 cm^{-1} to 3600 cm^{-1}, a broad and strong peak appeared in the FTIR curve of PLA, which corresponded to the stretching vibration absorption peak of the free bond O-H group, while the C = O stretching vibration absorption of the PLA ester group appeared near 1754cm^{-1}. For HBPA/PLA blends, with the increase of HBPA content, two absorption peaks appeared at the hydroxyl stretching vibration absorption peak at around 3500 cm^{-1}, and the bending vibration absorption peak of the O-H group at 1379 cm^{-1} also had two absorption peaks, which were all due to the influence of the hydrogen bond between the amide bond in HBPA and the terminal amino group and PLA[24]. Therefore, the FTIR spectra of the blends showed that there were hydrogen bonds between HBPA and PLA.

3.5 Gel content characterization of PLA/HBPA blends

Gel content was a common method to characterize the degree of crosslinking of polymers. The non-crosslinked part of the polymer matrix can be dissolved with a solvent, and the remaining material was the crosslinked part. Then the gel content in the polymer matrix can be calculated. Figure 3(b) showed the results of the gel content of the HBPA/PLA blend. It can be seen that the gel content increased with the increase of the HBPA content. Cross-linking degree can reach 18.37% when the content of HBPA was 1.2phr, which fully proved the chemical cross-linking between HBPA and PLA, and provided strong evidence for the enhancement of PLA/HBPA.

3.8 SEM characterization of PLA/HBPA blends

Figure 4 showed the SEM images of PLA blends with different HBPA content. It can be seen from the figure that the impact fracture surface of pure PLA was smooth, which was a typical brittle fracture. With the addition of HBPA, the fracture surface was no longer smooth, it showed ductile fracture, especially the fracture surface of the blends with 1.0phr HBPA and the blends with 1.2phr HBPA appeared filamentous. More filaments can be seen in the SEM images of the blends with 1.0phr HBPA in Fig. 6(e), indicating that HBPA had a cross-linking effect in PLA. For the blends with 1.2phr HBPA, HBPA was still evenly distributed, and there was obvious wire drawing. After the HBPA content was higher than 1.0phr, the drawing phenomenon and a large number of small particles appeared at the same time. These small particles were the result of the agglomeration of HBPA. The fracture surface gradually smoothed, the performance of ductile fracture disappeared, and the ductile fracture began to transform to brittle fracture, which was in line with the test results of mechanical properties discussed below.

3.6 Rheological characterization of PLA/HBPA blends

Figure 5(a) shows the change of complex viscosity with frequency of blends with different HBPA content in the molten state. After adding HBPA, the overall melt viscosity had been greatly increased, the trend was that first increased and then decreased, and the blend with 1.0phr HBPA was the highest, indicating that HBPA did have a physical effect in the matrix. The reason was concluded from the SEM images. When HBPA was added at 1.0phr or more, agglomeration began to occur. After agglomeration, the effect of rigid spherical particles in PLA decreased, so the viscosity began to decrease.

Figure 5(b) shows the variation of storage modulus with frequency for blends with different HBPA content in the molten state. After adding HBPA, the storage modulus of the material was greatly increased, which reflected the increase in the melting elasticity of the material. With the increase of HBPA content, it showed a trend of first increasing and then decreasing. The trend was the same as above. When the HBPA content was higher than 1phr, the effect of HBPA will decrease due to the agglomeration.

Figure 5(c) shows the change of loss modulus with frequency of blends with different HBPA content. After adding HBPA, the loss modulus of the material was also greatly increased, reflecting the increase in the viscosity of the material. Therefore, due to the addition of HBPA, hydrogen bonding and physicochemical crosslinking made the melt viscoelasticity of the blend increase. The trend is the same as above, the highest was the blend with 1.0phr HBPA, then it was reduced due to HBPA agglomeration, corresponding to the tensile strength in the mechanical properties of this system. Therefore, the matrix can be reinforced by adding HBPA, because of the interaction between HBPA and the matrix.

Figure 5(d) shows the change of loss factor tan δ with frequency for blends with different HBPA content in the molten state. The tan δ decreased first and then increased with frequency, of which the blend with 1.0phr HBPA was the lowest. As is well known, when the storage modulus was much larger than the loss modulus, the material mainly undergone elastic deformation. When the loss modulus was much larger than the storage modulus, the material mainly undergone viscous deformation. HBPA reduced the overall tan δ of the material, which meant that the ratio of the storage modulus to the loss modulus of the material was reduced, indicating that the addition of HBPA had a greater impact on the viscous modulus

of the matrix. The role between the molecular chains in the polymer and between the HBPA was mainly to improve the viscosity of the matrix, so it showed that the effect of mechanics was that the toughness did not change much but the strength increased.

3.7 POM characterization of PLA/HBPA blends

Figure 6(a) showed the images of the initial crystallization of pure PLA. It can be seen that the crystal nuclei formed before the crystallization of pure PLA were less and unevenly distributed. The other images were POM images of the PLA/HBPA blends that crystallized completely within 30 minutes. In these images, when pure PLA was completely crystallized, the spherulites size was large but the number was small. With the increase of HBPA content, the size of spherulites first decreased and then increased, and the number of crystals increased first and then decreased. Among them, the blend with 0.8phr HBPA and the blend with 1.0phr HBPA were the most obvious, the good distribution and dispersion of HBPA acted as a heterogeneous nucleating agent of PLA and induced crystallization. Therefore, the number of spherulites increased and the size was reduced due to the same space. Later, due to the high content of HBPA, the agglomeration of HBPA led to poor distribution and dispersion. The agglomerated HBPA only occupied a little space, so the effect of the nucleating agent was weakened, and the spherulites where there was no HBPA acting as a nucleating agent return to their original size. The POM images showed that the blends with 0.8phr HBPA and the blends with 1.0phr HBPA had the best dispersion of HBPA.

3.9 Thermal characterization of PLA/HBPA blends

Figure 8(a) showed the DSC curve of the blend after adding different amounts of HBPA. Table 1 showed the glass transition temperature (T_g), cold crystallization temperature (T_{cc}), cold crystallization enthalpy (ΔH_{cc}), fusion enthalpy (ΔH_m), crystallinity (χ_c) and decomposition temperature(T_d) of blends with different HBPA content. It can be seen that the T_g of pure PLA was 60.3°C, and its T_{cc} was 117.3°C, and its χ_c is 4.22%. With the addition of HBPA, the T_g of the blends was maintained at about 60°C, and the cold crystallization temperature first increased and then decreased. The highest temperature rose to 120.3°C, and the lowest temperature dropped to 112.8°C, which indicated that the steric hindrance caused by a large number of benzene rings affected the movement of the PLA molecular chain, at the same time, the hydrogen bonds and micro-crosslinking were also factors that affect the movement of the PLA molecular chain when the content of HBPA was small, so the crystallization of PLA became difficult. While the HBPA content increased, due to the agglomeration of spherical HBPA resulting in lubrication, the molecular chain was easy to move and crystallization becomes easier, so the cold crystallization of PLA temperature decreases. And the addition of HBPA had no obvious effect on the crystallinity of PLA during heating. On the one hand, since the crystallinity of pure PLA was very low during the heating process, the effect of HBPA on the crystallization of PLA cannot be reflected in the heating process. The specific impact can be referred to the POM photo during the isothermal crystallization process below. On the other hand, the addition of HBPA was very low and will not have a significant effect on the crystallinity of PLA.

Figure 8 (b) showed the TGA curve of the blend after adding different amounts of HBPA. The initial decomposition temperature ($T_{5\%}$) of pure PLA was 358.9°C, $T_{50\%}$ was 387.3°C, and the temperature at complete decomposition ($T_{99\%}$) was 619.6°C. After adding HBPA, the decomposition curve was divided into two stages. Between 300°C and 400°C was the decomposition of the uncrosslinked part of PLA, and after 400°C was the decomposition of the crosslinked part of PLA. With the addition of HBPA, the decomposition temperature of PLA decreased and then recovered, indicating that the dispersion and distribution of HBPA had a certain influence on the thermal stability of PLA. The minimum was that the blend with a content of 1.0phr drops to 383.8°C. The reason was that the better the dispersion of HBPA, the greater the impact on the bonding energy of PLA. Because the uncrosslinked part of the PLA internal molecular chain forging was affected by the hydrogen bond generated by HBPA, the bond energy was reduced, and the initial decomposition temperature was slightly reduced. When the decomposition reached the cross-linked part, the bond energy of the cross-linked part was larger, so the energy required for decomposition was higher. From the point of view of the integral area of the decomposition curve in the second stage, the component with the highest degree of crosslinking was the blend with 1.2phr HBPA.

Table 1
Thermal parameters of HBPA/PLA blend.

HBPA content (phr)	T_g (°C)	T_{cc} (°C)	ΔH_{cc} (J/g)	ΔH_m (J/g)	χ_c (%)	$T_{5\%}$ (°C)	$T_{50\%}$ (°C)	$T_{99\%}$ (°C)	HDT (°C)
0	60.3	117.3	34.69	38.75	4.22	358.9	387.3	619.6	58.7
0.4	60.0	118.8	32.27	36.24	4.12	358.1	386.7	588.3	59.6
0.8	62.1	120.3	29.48	33.64	4.32	355.2	386.2	683.2	60.2
1.0	61.4	118.5	30.24	34.31	4.23	349.5	383.8	680.8	61.2
1.2	61.1	112.8	29.93	34.17	4.40	356.5	386.5	682	59.3

3.10 HDT characterization of PLA/HBPA blends

It can be seen from Table 1 that the thermal deformation temperature of PLA also rose with the addition of HBPA, which proved that the addition of HBPA can effectively strengthen the PLA and made the PLA composite material difficult to deform. PLA had the best reinforcing effect when the content of HBPA was 1.0phr. After the addition amount of HBPA exceeded 1 phr, the reinforcing effect was slightly reduced because HBPA was easy to agglomerate.

3.11 Mechanical characterization of PLA/HBPA blends

Figure 8(a) showed the mechanical properties of PLA blends with different contents of HBPA. It can be seen intuitively that the tensile strength first increased and then decreased. The blends with 1.0phr HBPA showed the best tensile strength. Compared with the pure PLA (42.57 MPa), the tensile strength of the

blends with 1.0phr HBPA (60.36MPa) increased by 41.79%. The elongation at break was almost a smooth straight line, which was basically maintained at about 1.8%. The impact strength curve was consistent with the elongation at break. The above results showed that adding an appropriate amount of HBPA modifier can increase the strength of the blend. The difference from other inorganic fillers was that inorganic fillers will reduce toughness while strengthening.

Figure 8(b) was the stress-strain curves of PLA/HBPA blends. It can be seen from the figure that the strength of PLA had been significantly improved after adding HBPA, and the strain was always around 1.8%. With the increase of HBPA content, the strength first increased and then decreased, and reaching the maximum when HBPA content was 1.0phr. Figure 8(c) was the integral area under the stress-strain curve of the PLA blends with different contents of HBPA, which was the tensile fracture energy(U_E). Figure 8(d) showed that the changes of tensile modulus with increasing HBPA content. As can be seen in the two figures, the U_E and elastic modulus were both improved after adding HBPA, and both reaching the maximum when HBPA content was 1.0phr.

The mechanical properties test of the blends showed that HBPA had successfully enhanced PLA, and the increase in fracture energy indicated the transition of the blend from brittle fracture to ductile fracture. The reason was that HBPA contained a large number of benzene rings, which can provide a certain rigidity to PLA. Secondly, HBPA molecule terminal contained a large number of amine groups, which can have strong hydrogen bonding with the hydroxyl and carboxyl groups (containing active hydrogen atoms) of the PLA resin, which enhanced the force between the PLA molecules. In addition, due to the special structure of HBPA, such as high degree of branching, active amide bonds on the branch chain and active terminal amine groups can be used for the chemical action of the groups on the PLA molecular chain, and form physical and chemical interactions. Therefore, it also improved the strength of PLA. The distribution of HBPA in PLA can theoretically provide the strength and toughness of the matrix at the same time[28]. On the one hand, because HBPA contained a large number of cavities that can provide energy absorption, on the other hand, the cross-linking effect also improved the toughness to a certain extent. The benzene ring itself had a strong steric hindrance, and the spherical structure of HBPA led to easy agglomeration, which will have a certain adverse effect on the toughness of PLA. In the research, the amount of HBPA added was small. In the case of a small amount, so HBPA had made a valuable contribution to the improvement of the mechanical properties of PLA.

4 Conclusions

In this work, trimesoyl chloride and p-phenylenediamine were used as monomers to successfully synthesize amine-terminated hyperbranched polymers. Through characterizations, its groups and structure were determined, which was proved that the polymers was third-generation and fourth-generation dendritic hyperbranched polyamide. FTIR spectrum showed that there were hydrogen bonds between HBPA and PLA. The test results of gel content showed that HBPA and PLA were chemically cross-linked. The filamentous phenomenon in the SEM images indicated that cross-linking occurs, and the spherical particles indicated agglomeration. The studies of thermal performance showed the addition

of HBPA had a greater impact on the viscous modulus of the matrix. HBPA would act as a nucleating agent of PLA during the isothermal process. HBPA did not affect the Tg and crystallinity of PLA. The slight increase in the cold crystallization temperature indicated that the blends were difficult to crystallize under the conditions of good dispersion of HBPA in PLA. After HBPA was added, the blend had two thermal decomposition stages, namely the uncrosslinked part and the crosslinked part. And the addition of HBPA can increase the heat distortion temperature of PLA. The mechanical test results of the HBPA/PLA blend showed that the addition of HBPA to PLA can increase the strength of PLA. The increase in tensile strength was up to 41.8%. In summary, HBPA was an effective additive to enhance PLA.

Declarations

Acknowledgement

The authors are grateful to the support of National Natural Science Youth Foundation (51503007), Beijing Young Top-notch Personnel Foundation(CIT&TCD201804030), 2021 Postgraduate Research Ability Improvement Program Project (Beijing Technology and Business University, Beijing 100048, China). Also, we acknowledge Beijing Key Laboratory of Quality Evaluation Technology for Hygiene and Safety of Plastics for the award of an Open Fund (QETHSP2020013).

References

1. Ferreira EDB, Luna CBB, Siqueira DD, Araujo EM, de Franca DC, Wellen RMR (2021) Annealing Effect on Pla/Eva Blends Performance. J Polym Environ: 1–14
2. Perin D, Rigott D, Fredi G, Papageorgiou GZ, Bikiaris DN, Dorigato A (2021) Innovative Bio-based Poly(Lactic Acid)/Poly(Alkylene Furanoate)s Fiber Blends for Sustainable Textile Applications. J Polym Environ: 1–16
3. Deeksha B, Sadanand V, Hariram N, Rajulu AV (2021) Preparation and properties of cellulose nanocomposite fabrics with in situ generated silver nanoparticles by bioreduction method. J Bioresour Bioprod 6:75–81
4. Ashok B, Hariram N, Siengchin S, Rajulu AV (2020) Modification of Tamarind Fruit Shell Powder with In Situ Generated Copper Nanoparticles by Single Step Hydrothermal Method. J Bioresour Bioprod 5:180–185
5. Rani S, Kumar KD, Mandal S, Kumar R (2020) Functionalized carbon dot nanoparticles reinforced soy protein isolate biopolymeric film. J Polym Res 27:312
6. Quiles-Carrillo L, Blanes-Martínez MM, Montanes N, Fenollar O, Torres-Giner S, Balart R (2018) Reactive toughening of injection-molded polylactide pieces using maleinized hemp seed oil. Eur Polym J 98:402–410
7. Lamparelli RDBC, Montagna LS, da Silva APB, Montanheiro TLD, Lemes AP (2021) Study of the Biodegradation of PLA/PBAT Films after Biodegradation Tests in Soil and the Aqueous Medium.

Biointerface Res App 12:833–846

8. Silva APB, Montagna LS, Passador FR, Rezende MC, Lemes AP (2021) Biodegradable nanocomposites based on PLA/PHBV blend reinforced with carbon nanotubes with potential for electrical and electromagnetic applications. Express Polym Lett 15:987–1003
9. Zheng HJ, Sun ZQ, Zhang HJ (2020) Effects of walnut shell powders on the morphology and the thermal and mechanical properties of poly(lactic acid). J Thermoplast Compos Mater 33:1383–1395
10. Foglia F, De Meo A, Iozzino V, Volpe V, Pantani R (2020) Isothermal crystallization ofPLA: Nucleation density and growth rates of alpha and alpha' phases. Can J Chem Eng 98:1998–2007
11. Saki Z, Azizi H, Ghasemi I et al. Morphology development to achieve electrical conductive blends based on polylactic acid/polyolefin elastomer/graphene nanoplates[J]. Express Polymer Letters, 2021, 15(10)
12. Michalski A, Brzezinski M, Lapienis G, Biela T (2019) Star-shaped and branched polylactides: Synthesis, characterization, and properties. Prog Polym Sci 89:159–212
13. Irska I, Linares A, Piesowicz E, Paszkiewicz S, Roslaniec Z, Nogales A, Ezquerra TA (2019) Dielectric spectroscopy of novel bio-based aliphatic-aromatic block copolymers: Poly(butylene terephthalate)-b-poly(lactic acid). Eur Phys J E Soft Matter 42:107
14. Aliotta L, Cinelli P, Coltelli MB, Lazzeri A (2019) Rigid filler toughening in PLA-Calcium Carbonate composites: Effect of particle surface treatment and matrix plasticization. Eur Polym J 113:78–88
15. Wang QQ, Ji CC, Sun JZ, Yao Q, Liu J, Saeed RMY (2019) Kinetic thermal behavior of nanocellulose filled polylactic acid filament for fused filament fabrication 3D printing. J Appl Polym Sci 137:48374
16. Frone AN, Batalu D, Chiulan I, Oprea M, Gabor AR, Nicolae CA, Raditoiu V, Trusca R, Panaitescu DM (2019) Morpho-Structural, Thermal and Mechanical Properties of PLA/PHB/Cellulose Biodegradable Nanocomposites Obtained by Compression Molding, Extrusion, and 3D Printing. Nanomaterials (Basel) 10:51
17. Kilic NT, Can BN, Kodal M, Ozkoc G (2019) Compatibilization of PLA/PBAT blends by using Epoxy-POSS. J Appl Polym Sci 136:47217
18. Rigoussen A, Raquez JM, Dubois P, Verge P (2019) A dual approach to compatibilize PLA/ABS immiscible blends with epoxidized cardanol derivatives. Eur Polym J 114:118–126
19. Zhang M, Ding XQ, Zhan YX, Wang YT, Wang XL (2020) Improving the flame retardancy of poly(lactic acid) using an efficient ternary hybrid flame retardant by dual modification of graphene oxide with phenylphosphinic acid and nano MOFs. J Hazard Mater 384:121260
20. Scaffaro R, Maio A, Nostro A (2020) Poly(lactic acid)/carvacrol-based materials: preparation, physicochemical properties, and antimicrobial activity. Appl Microbiol Biotechnol 104:1823–1835
21. Li YY, Rong JX, Zhang QX (2020) Preparation and properties of citric acid modified calcium carbonate/polylactic acid composites. China Plastics 38:165–168
22. Song ZY, Li NZ, Zhang L, Li J (2020) The effect of modified silica on the properties of SiO2/PLA composite film. China Plastics 41:142–148

23. Li SP, Lin Q, Lv TT, Li YB, Hou HJ, Zhu HJ, Wu QS, Cui C (2016) Synergic improvement of DGEBA/CSP/HBP composite on mechanical behavior. Polym Sci Ser A 58:785–792
24. Lin Y, Zhang KY, Dong ZM, Dong LS, Li YS (2007) Study of Hydrogen-Bonded Blend of Polylactide with Biodegradable Hyperbranched Poly(ester amide). Macromolecules 40:6257–6267
25. Chen SF, Xu ZJ, Zhang DH (2018) Synthesis and application of epoxy-ended hyperbranched polymers. Chem Eng J 343:283–302
26. Han XL, Jin YJ, Wang BH, Tian HF, Weng YX (2021) Reinforcing and Toughening Modification of PPC/PBS Blends Compatibilized with Epoxy Terminated Hyperbranched Polymers. J Polym Environ 12
27. Wang B, Jin YJ, Kang KE, Yang N, Weng YX, Huang ZG, Men S (2020) Investigation on compatibility of PLA/PBAT blends modified by epoxy-terminated branched polymers through chemical micro-crosslinking. e-Polymers 20:39–54
28. Luan YG, Zhang XA, Jiang SL, Chen JH, Lyu YF (2018) Self-healing Supramolecular Polymer Composites by Hydrogen Bonding Interactions between Hyperbranched Polymer and Graphene Oxide. Chin J Polym Sci 36:584–591
29. Fei XM, Wei W, Tang YY, Zhu Y, Luo J, Chen MQ, Liu XY (2017) Simultaneous enhancements in toughness, tensile strength, and thermal properties of epoxy-anhydride thermosets with a carboxyl-terminated hyperbranched polyester. Eur Polym J 90:431–441
30. Ma C, Qiu SL, Yu B, Wang JL, Wang CM, Zeng WR, Hu Y (2017) Economical and environment-friendly synthesis of a novel hyperbranched poly(aminomethylphosphine oxide-amine) as co-curing agent for simultaneous improvement of fire safety, glass transition temperature and toughness of epoxy resins. Chem Eng J 322:618–631
31. Ma C, Qiu SL, Wang JL, Sheng HB, Zhang Y, Hu WZ, Hu Y (2018) Facile synthesis of a novel hyperbranched poly(urethane-phosphine oxide) as an effective modifier for epoxy resin. Polym Degrad Stabil 154:157–169
32. Chen J, Nie XA, Jiang JC (2020) Synthesis of a Novel Bio-Oil-Based Hyperbranched Ester Plasticizer and Its Effects on Poly(vinyl chloride) Soft Films. ACS Omega 5:5480–5486
33. Wang DL, Jin Y, Zhu XY, Yan DY (2017) Synthesis and applications of stimuli-responsive hyperbranched polymers. Prog Polym Sci 64:114–153

Figures

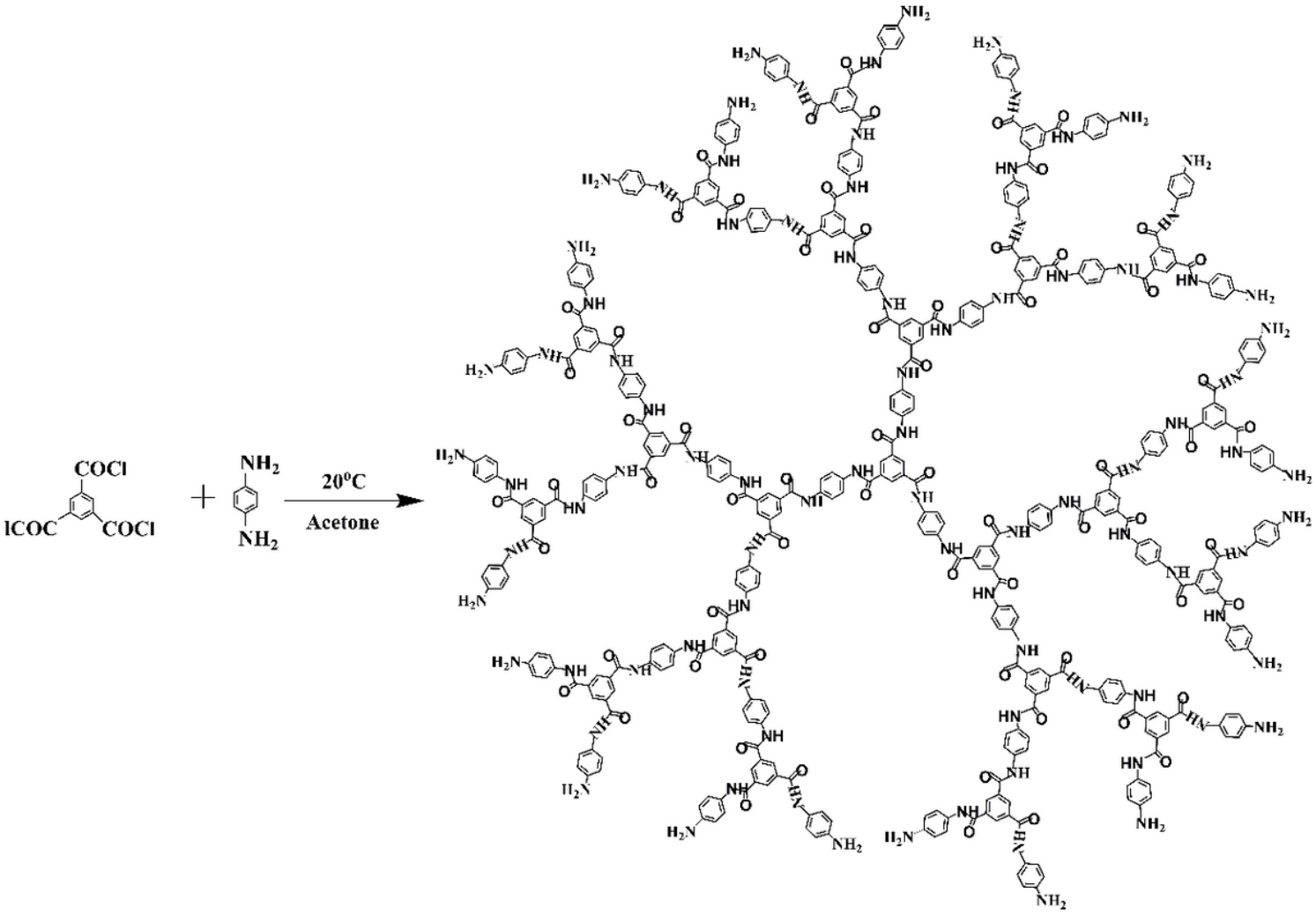

Figure 1

Synthesis process of the four generation HBPA

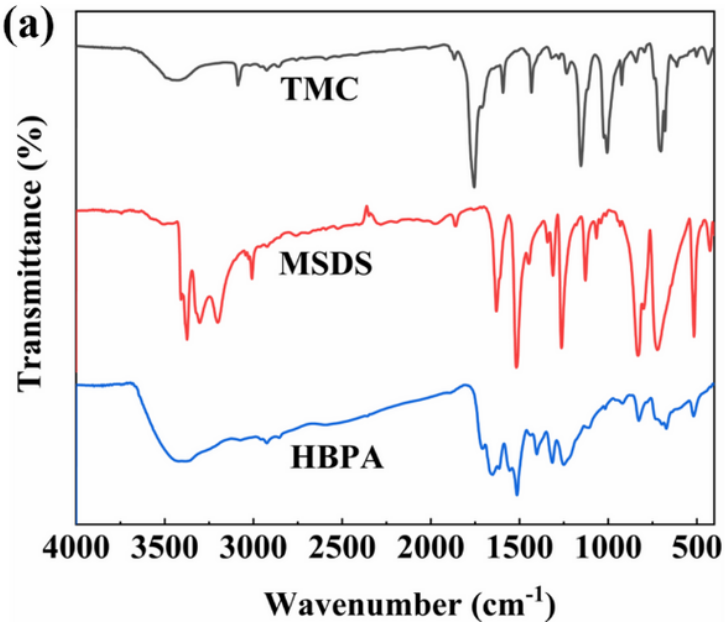

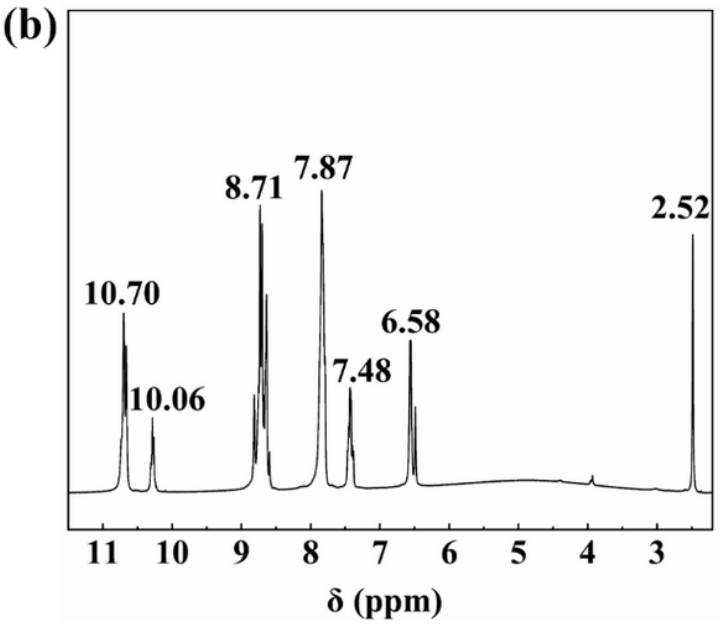

Figure 2

Structure characterization of HBPA. (a) FTIR spectra. (b)The 1H-NMR spectrum.

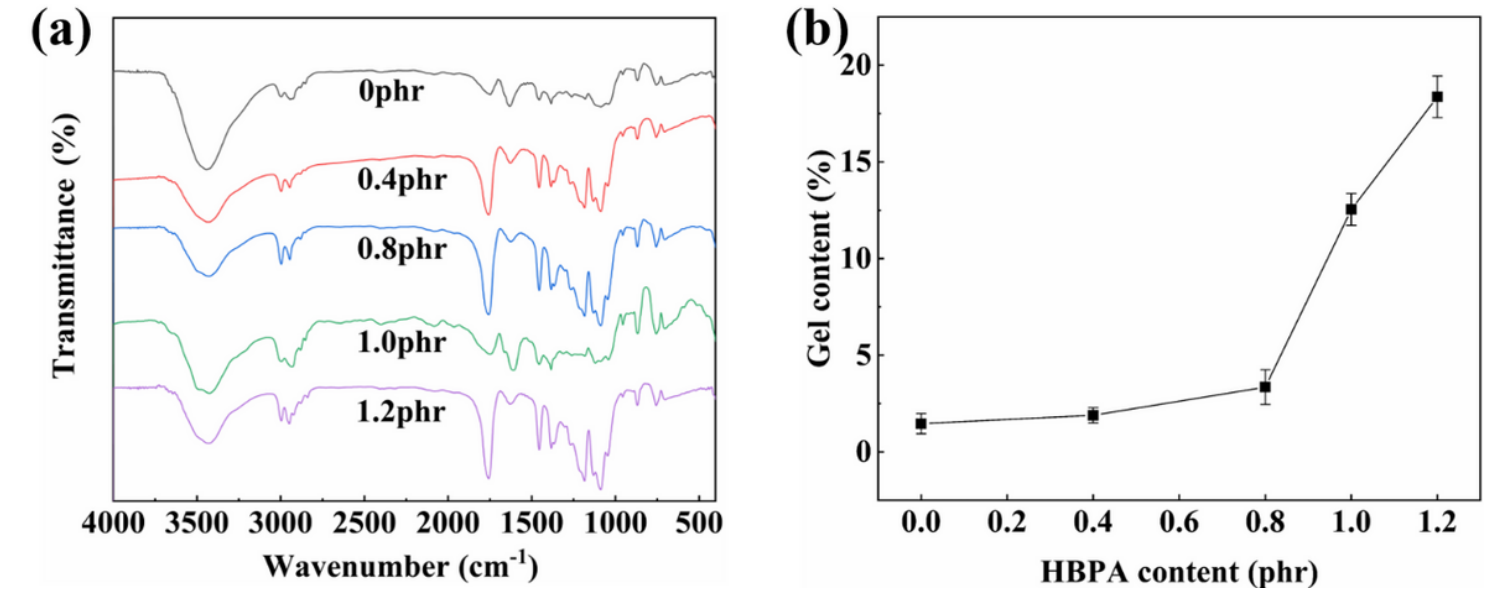

Figure 3

Characterization of intermolecular interactions of blends. (a)FTIR spectra of PLA blends with different contents of HBPA. (b)The gel content of HBPA/PLA blends.

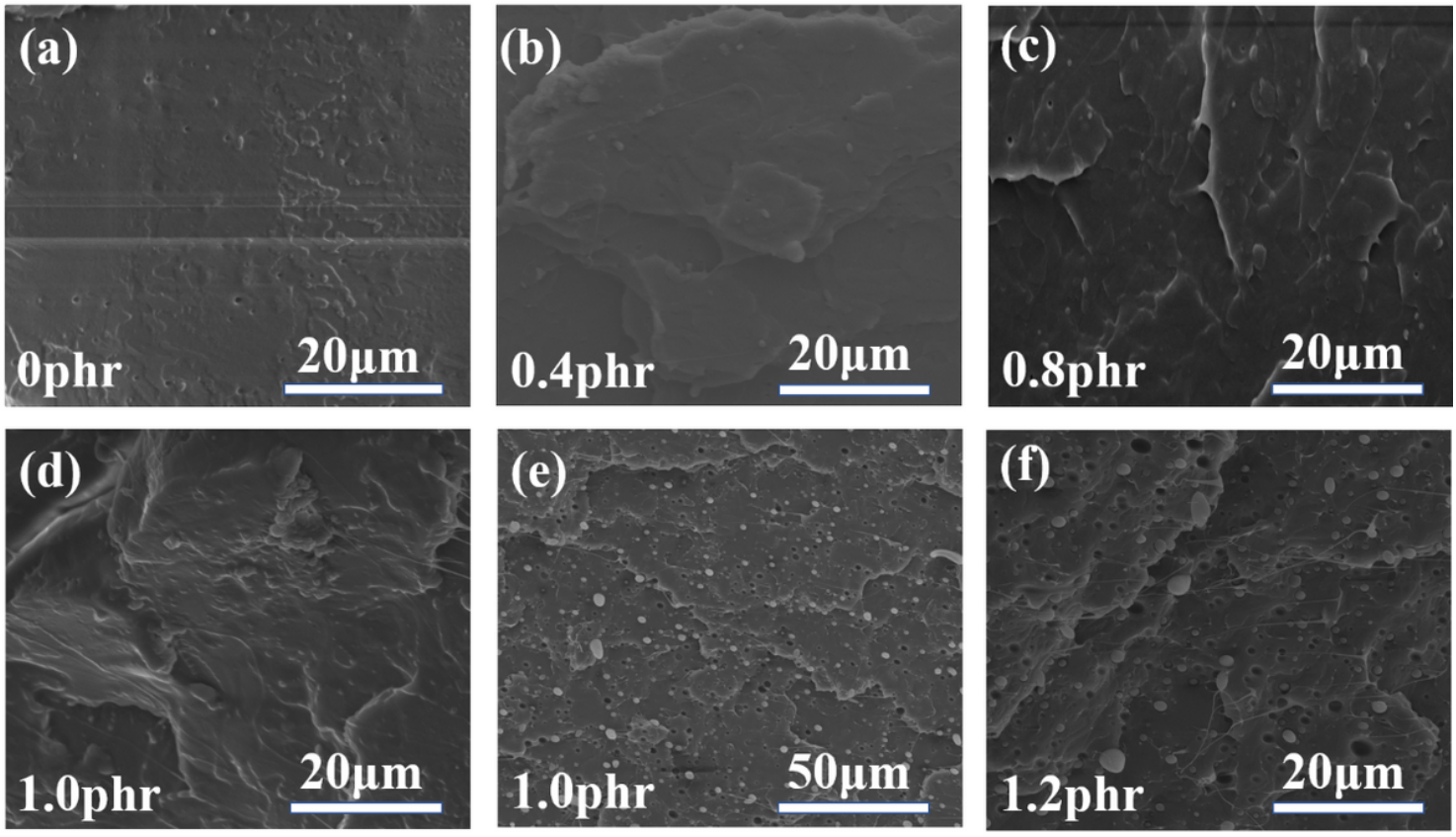

Figure 4

SEM images of PLA/HBPA blends

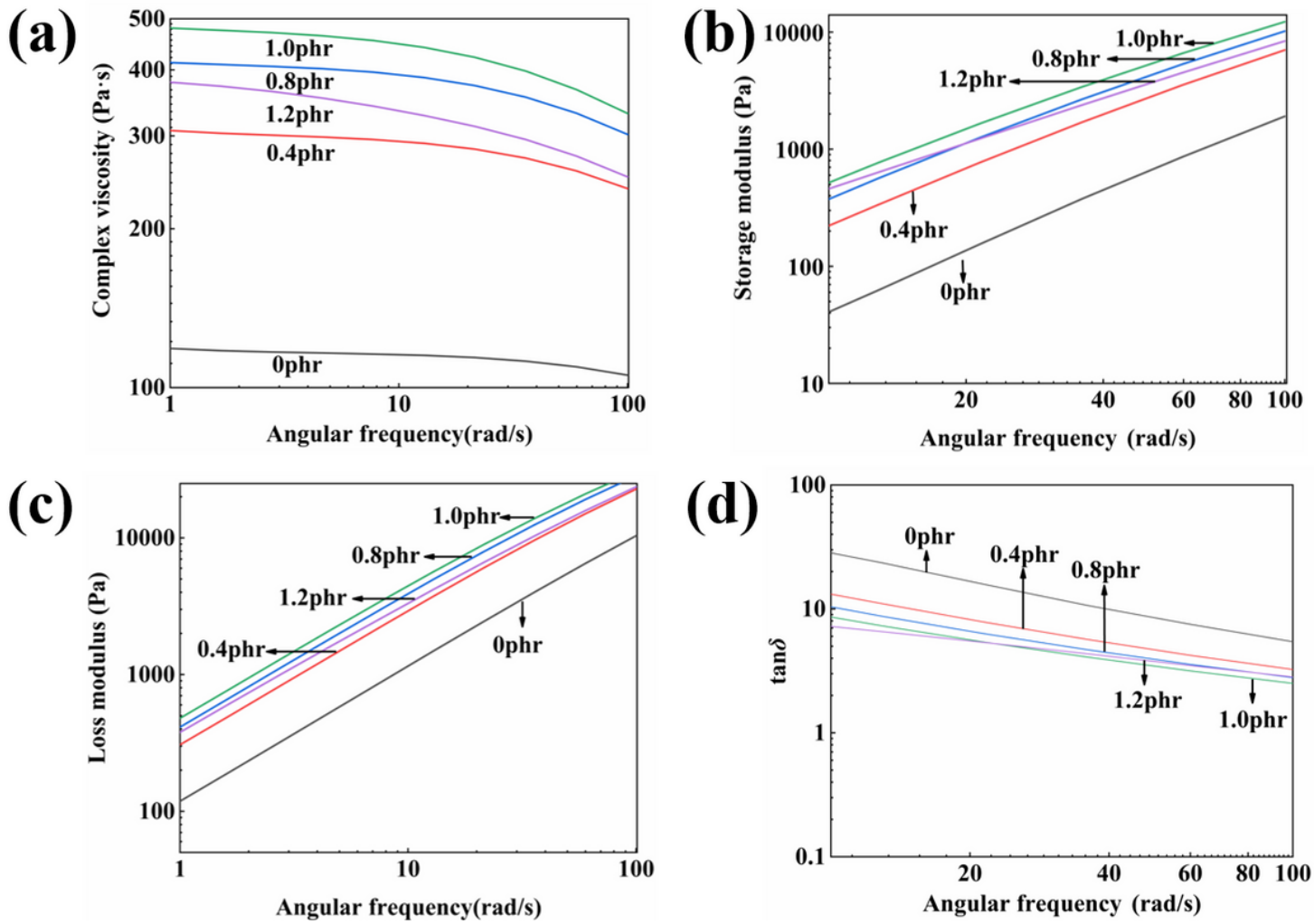

Figure 5

Rheological characterization of blends. (a)The composite viscosity diagrams of HBPA/PLA; (b)The storage modulus diagram of HBPA/PLA; (c)The loss modulus diagram of HBPA/PLA.; (d)The loss factor graph of HBPA/PLA

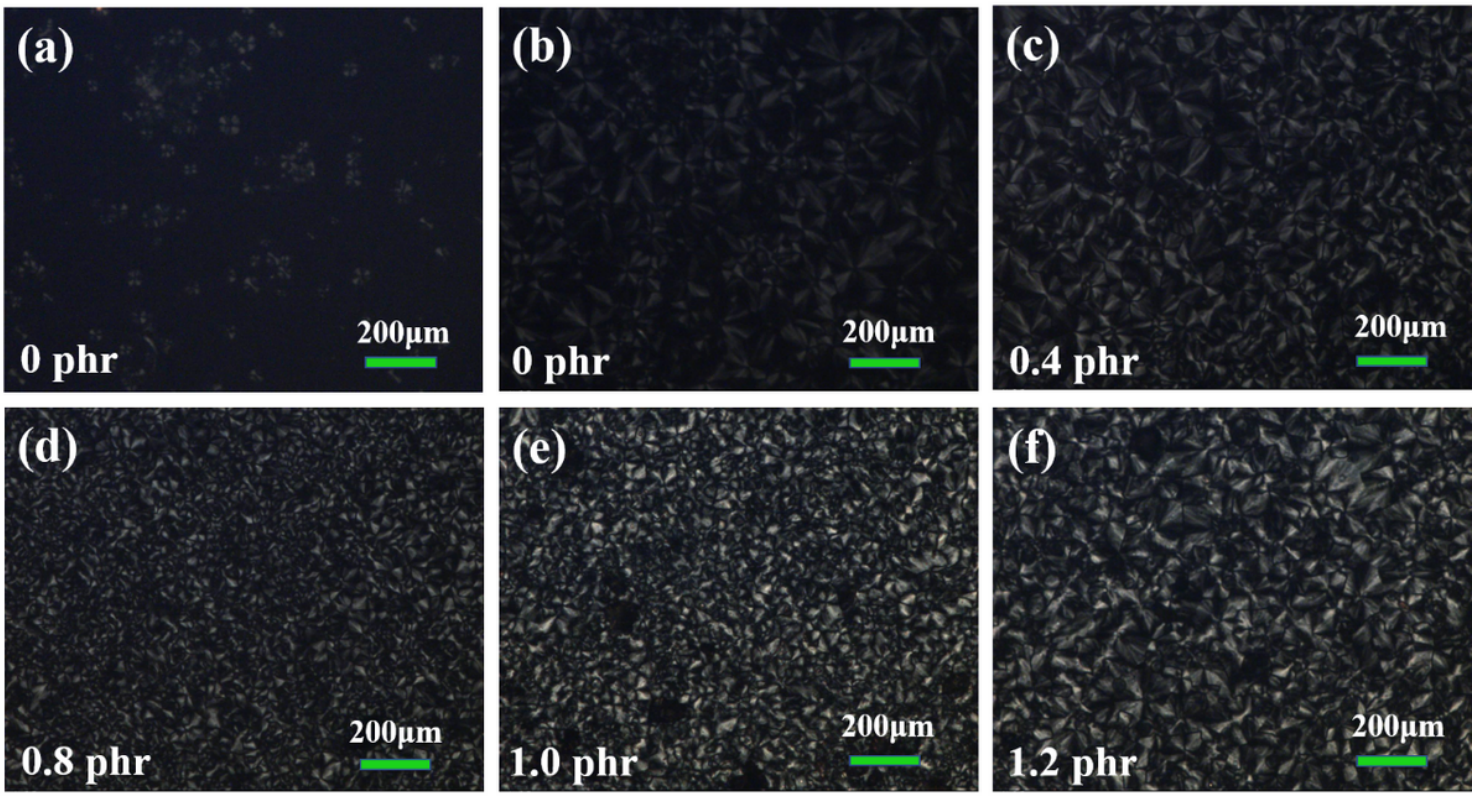

Figure 6

Isothermal crystallization POM images of PLA blends with different contents of HBPA at 120 °C.

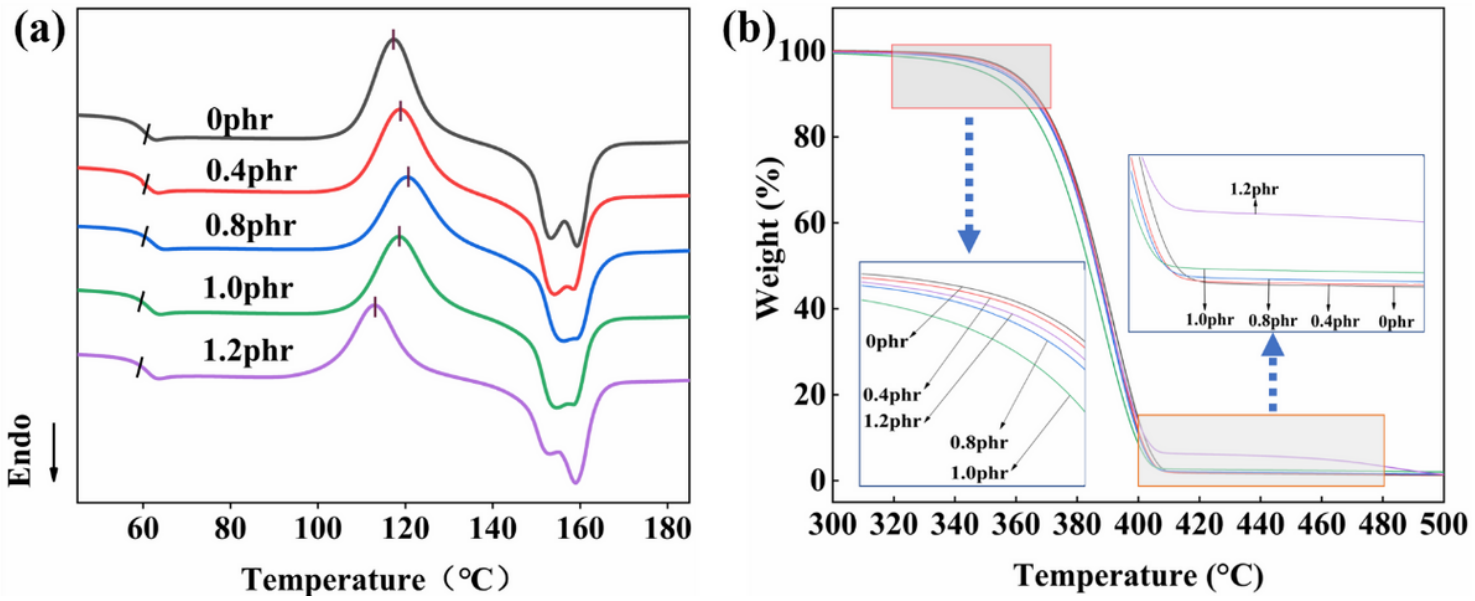

Figure 7

Thermal characterization of blends. (a) DSC curves of HBPA/PLA blend. (b) TGA curves of HBPA/PLA blend.

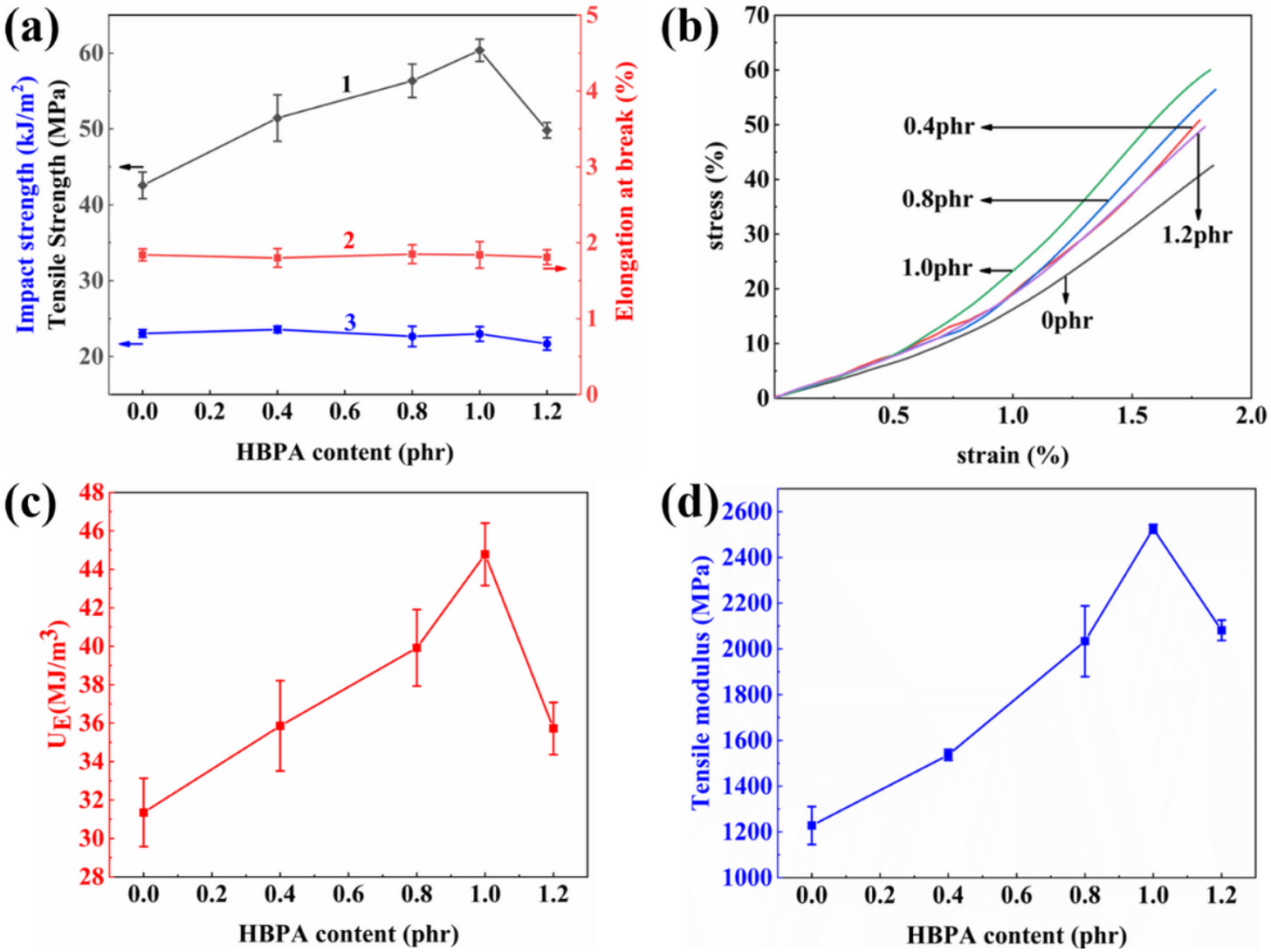

Figure 8

Mechanical properties. (a) 1-Tensile strength; 2-elongation at break; 3-impact strength. (b) Stress-strain curves of PLA/HBPA blends. (c) Fracture energy (UE) of PLA/HBPA blends. (d) Tensile Modulus of PLA/HBPA blends.